Magnetic structure of greigite (Fe_3S_4) probed by neutron powder diffraction and polarized neutron diffraction

Liao Chang,[1] Brian D. Rainford,[2] J. Ross Stewart,[3] Clemens Ritter,[3] Andrew P. Roberts,[1] Yan Tang,[4] and Qianwang Chen[4]

Received 17 December 2008; revised 15 April 2009; accepted 24 April 2009; published 11 July 2009.

[1] We have investigated greigite (Fe_3S_4) using a combination of neutron powder diffraction and polarized neutron diffraction to give the first unambiguous assignment of its magnetic structure. Our results confirm that greigite has a collinear ferrimagnetic structure with antiferromagnetic coupling between the tetrahedral (*A*) and octahedral (*B*) sites. Our analysis also indicates that greigite does not have a significant vacancy concentration or spin canting. High-resolution neutron powder diffraction results enable determination of sublattice magnetizations of the *A* and *B* sites. At room temperature, the average magnetic moments on the two sites are almost the same ($\sim$3.0 μ_B), with a net magnetic moment of $\sim$3.0 μ_B per formula unit (fu). The magnetic moment of the *B* sites decreases slightly between 10 K and room temperature, while the *A* site moment is relatively stable as a function of temperature; this indicates that greigite is probably an R-type ferrimagnet. At 10 K, the average magnetic moments of the *A* and *B* sites are 3.0 μ_B and 3.25 μ_B, respectively. Neutron diffraction measurements, coupled with magnetic measurements, on our pure synthetic greigite samples indicate that the saturation magnetization of greigite is lower than that of magnetite (Fe_3O_4). It is proposed that the lower magnetic moment in greigite (saturation magnetization is $\sim$59 A m^2 kg^{-1}) compared to magnetite is probably caused by an increased degree of covalency between iron and sulfur compared to oxygen ligands or by greater delocalization of the 3*d* electrons in greigite.

Citation: Chang, L., B. D. Rainford, J. R. Stewart, C. Ritter, A. P. Roberts, Y. Tang, and Q. Chen (2009), Magnetic structure of greigite (Fe_3S_4) probed by neutron powder diffraction and polarized neutron diffraction, *J. Geophys. Res.*, *114*, B07101, doi:10.1029/2008JB006260.

1. Introduction

[2] Greigite (Fe_3S_4) is an iron thiospinel, which has the same crystal structure as magnetite (Fe_3O_4) [*Skinner et al.*, 1964]. Greigite crystallizes in the inverse spinel structure (space group $Fd\bar{3}$ m, Z = 8). As the basic phase in the thiospinel family, its unique magnetic and electronic properties have attracted considerable interest in solid state physics and chemistry [e.g., *Coey et al.*, 1970; *Yamaguchi and Wada*, 1970; *Spender et al.*, 1972; *Goodenough and Fatseas*, 1982; *Braga et al.*, 1988; *Letard et al.*, 2005]. More importantly, greigite has been increasingly recognized to be geologically and geophysically important since its formal identification in lacustrine sediments [*Skinner et al.*, 1964] and in anaerobic magnetotactic bacteria [e.g., *Farina et al.*, 1990; *Mann et al.*, 1990]. It is now recognized that greigite is widely distributed in marine and lake sediments, in which anoxic, sulfate-reducing diagenetic conditions have occurred [e.g., *Roberts and Weaver*, 2005, and references therein]. Its presence within sediments can therefore significantly affect paleomagnetic and environmental magnetic records.

[3] Despite its importance and widespread occurrence in natural environments, many magnetic properties of greigite remain unknown because of its metastability [e.g., *Berner*, 1984; *Rickard and Luther*, 2007]. This sulfide phase is prone to oxidize in air, decompose at elevated temperatures, and react to form other iron sulfides. The greigite produced in many syntheses is affected by impurities, lattice defects and small grain size, which leads to superparamagnetic (SP) effects. Difficulty in obtaining pure greigite samples has also hindered determination of many important magnetic properties of greigite. An ongoing problem has been that the magnetic structure of greigite is still not clear, although its crystal structure has been well established [e.g., *Skinner et al.*, 1964]. It has been presumed that greigite has the same magnetic structure as magnetite because of their similar crystallographic structure. However, previous studies indi-

[1]National Oceanography Centre, University of Southampton, European Way, Southampton, UK.
[2]School of Physics and Astronomy, University of Southampton, Southampton, UK.
[3]Institut Laue-Langevin, Grenoble, France.
[4]Hefei National Laboratory for Physical Sciences at Microscale and Department of Materials Science and Engineering, University of Science and Technology of China, Hefei, China.

0148-0227/09/2008JB006260$09.00

cate that the saturation magnetization (M_s) of greigite appears to be much smaller than that of magnetite [e.g., *Uda*, 1965; *Coey et al.*, 1970; *Spender et al.*, 1972; *Hoffmann*, 1992; *Reynolds et al.*, 1994; *Dekkers and Schoonen*, 1996; *Chen et al.*, 2005; *He et al.*, 2006]. Various models have been proposed to account for the electronic and magnetic structures of greigite [e.g., *Coey et al.*, 1970; *Spender et al.*, 1972; *Goodenough and Fatseas*, 1982; *Braga et al.*, 1988; *Sherman*, 1990; *Letard et al.*, 2005]. On the basis of Mössbauer spectroscopy measurements, *Coey et al.* [1970] proposed that greigite had the same ferrimagnetic structure as magnetite, but the expected net magnetic moment of ≥ 4 μ_B (considering the spin-only values for ionic moments in the Néel model) was inconsistent with their low measured magnetic moment (2.2 ± 0.2 μ_B fu^{-1}, extrapolated to 0 K). Magnetic measurements on the purest known synthetic greigite samples give the most accurate available M_s estimate of $\sim$59 A m^2 kg^{-1} (3.1 μ_B fu^{-1}) [*Chang et al.*, 2008]. While the low M_s values reported in most published studies of greigite are largely caused by sample impurity, this recently reported M_s value is still inconsistent with the assumed high-spin ionic model for greigite [*Chang et al.*, 2008]. It has also been speculated that the (Fe^{2+}, Fe^{3+}) distribution in greigite is different from magnetite, that the magnetic state of these ions is different, or that the magnetic structure is not the collinear ferrimagnetic structure found in magnetite.

[4] Production of pure, single-phase synthetic greigite samples makes it possible to establish some of its fundamental magnetic properties. In order to resolve the ambiguities associated with its magnetic structure, we have carried out a magnetic structure determination study using a combination of neutron powder diffraction (NPD) and polarized neutron diffraction on a highly pure synthetic greigite sample. Our analysis reveals the magnetic structure of greigite, along with the sublattice magnetizations and their temperature dependence, for the first time.

2. Samples and Experiments

[5] The synthetic greigite samples analyzed in this study were prepared by reacting ferric chloride ($FeCl_3 \cdot 6H_2O$) with thiourea (CH_4N_2S) and formic acid (HCOOH) at 170°C according to a new hydrothermal method [*Tang et al.*, 2007; *Chang et al.*, 2008]. The samples have been confirmed to be pure, single-phase greigite that occurs as large polycrystalline grains [*Chang et al.*, 2008]. Each synthesis yielded only less than 50 mg of pure greigite. Several tens of greigite syntheses were therefore carried out to provide enough material for this study. X-ray diffraction (XRD) analysis was carried out immediately after each synthesis to monitor sample purity. XRD spectra were recorded using a Phillips X'pert X-ray diffractometer with high-intensity Cu-Kα radiation (λ = 1.54056 Å) at a scanning speed of 0.05° s^{-1} over a 2θ range from 10 to 80°. Samples with mixed phases were rejected and were not used for further analysis. The main impurities are cubic pyrite (FeS_2), orthorhombic marcasite (FeS_2) and elemental sulfur (S). The resulting pure synthetic greigite samples ($\sim$20 batches with a total weight of $\sim$1 g) were kept in a desiccator to prevent wet oxidation before the neutron scattering experiments, which were conducted about half a year after synthesis. To enable cross comparison of data for our pure synthetic greigite, NPD analyses were also made for the three purest natural greigite samples in our sample collection. These include iron sulfide nodules from the Valle Ricca section, near Rome, Italy [*van Dongen et al.*, 2007] and from southwestern Taiwan [*Jiang et al.*, 2001], and a coarse-grained greigite sample from the Czech Republic [*Chang et al.*, 2007].

[6] Neutron powder diffraction experiments were carried out at the Institut Laue-Langevin (ILL), Grenoble, France. The diffraction patterns were collected using both the high-intensity neutron powder diffractometer D1B and the high-resolution neutron powder diffractometer D1A at ILL using neutron wavelengths of 2.51 Å and 1.91 Å, respectively. The sample was held in a vanadium can for the NPD experiments. Full diffraction patterns were measured on D1A at 10, 100, 200, and 290 K, with typical acquisition times of about 4 h per temperature. On D1B, with its banana multidetector, it took only $\sim$10 min to acquire a single diffraction pattern. Successive measurements were made as the temperature was slowly ramped between room temperature and 10 K. Polarized neutron diffraction experiments were performed using the neutron polarization analysis spectrometer D7 at ILL. The incident neutron beam, with wavelength of 3.1 Å, was polarized by a supermirror polarizer before being scattered by the sample. A vertical field of 5 T was applied to saturate the magnetization of the sample normal to the scattering plane. The magnetic anisotropy of greigite is low (the coercivity of the studied multidomain greigite sample is normally less than 10 mT at room temperature [*Chang et al.*, 2007, 2008]); therefore, the magnetic moment can be readily oriented along the applied field. While D7 is designed for full polarization analysis, this technique is not applicable to a ferromagnet or ferrimagnet. Instead we only measured the nonspin-flip scattering intensities I (+, +) and I (−, −), which correspond to the scattering intensities with the neutron spin parallel (flipper off) and antiparallel (flipper on) to the sample magnetization [*Moon et al.*, 1969]. A neutron spin-flipper was used to change the polarity of the neutron beam. The spin-flip scattering intensities (I (+, −) and I (+, −)) were not measured. To avoid analysis of the polarization of the scattered beam, a thin (0.1 mm) shim of unmagnetized iron was placed between the sample and the detector banks. This had the effect of depolarizing the scattered beam before it reached the polarizing analyzers in front of the D7 detectors. The sample was held in an aluminum sample can inside an ILL orange cryostat, allowing measurements between 2 K and room temperature. The incident neutron wavelength of 3.1 Å permitted the first 10 Bragg peaks to be measured.

3. Results

3.1. Neutron Powder Diffraction

[7] NPD is the primary technique for probing the magnetic structures of magnetic materials [e.g., *Rodríguez-Carvajal*, 1993]. The X-ray and neutron diffraction patterns for the synthetic greigite sample confirm the sample purity (Figure 1): all the peaks may be indexed in the $Fd\bar{3}$ m space group and there is no sign of significant impurity peaks. The purity of the analyzed synthetic sample is especially clear when plotted alongside data for the purest available natural samples (Figure 1), which commonly contain pyrite and

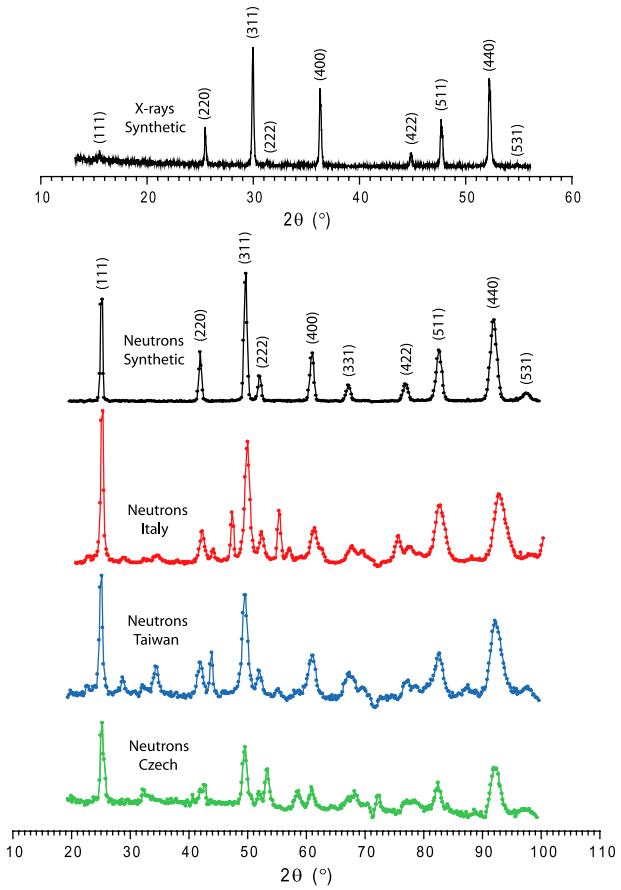

Figure 1. A room temperature X-ray diffraction pattern (λ = 1.54 Å) for the synthetic greigite sample is shown (top curve) for comparison with a room temperature neutron diffraction spectrum (bottom four curves) recorded on the high-intensity neutron powder diffractometer D1B (λ = 2.51 Å). A pronounced magnetic scattering contribution is observed in the neutron diffraction pattern, e.g., the (111), (222), and (331) reflections. NPD patterns are also shown for three natural greigite samples. The differences between these NPD patterns are attributed to impurities in the natural samples.

silicate grains in addition to greigite. The difference in relative intensities of the peaks between the X-ray and neutron data is partly due to the difference in atomic scattering amplitudes for X rays and neutrons, but there is also a large magnetic contribution in the neutron patterns. This is particularly evident in the (111), (222), (331), and (531) peaks. The data from D1B (Figure 1) are characteristic of a medium-resolution diffractometer, with the multidetector coverage extending over the first ten Bragg peaks. D1A is a high-resolution instrument, as can be seen from the narrow peak widths in Figure 2. Its shorter wavelength also allows a larger range of d spacings to be studied (28 peaks up to the maximum 2θ).

[8] For unpolarized neutrons diffracted from a ferromagnetic or ferrimagnetic sample, there is no coherence between the nuclear and magnetic diffraction. The total scattering intensity is therefore the sum of the nuclear and magnetic diffraction intensities. To analyze the diffraction patterns, we used a two-phase profile refinement method: one phase involves the nuclear scattering contribution, while the second involves the magnetic scattering contribution. Rietveld analysis was carried out using the FULLPROF suite [*Rodríguez-Carvajal*, 1993] (Figure 2) to refine a minimal set of variables, i.e., the lattice parameter, the internal sulfur coordinate u, and the magnetic moments of the tetrahedral and octahedral sites, as well as absorption, background, and profile coefficients (Table 1). The inverse spinel structure (space group $Fd\bar{3}$ m) refined from our NPD data agrees well with that determined by XRD [e.g., *Skinner et al.*, 1964; *Spender et al.*, 1972]. In this crystal structure, it is supposed that Fe^{3+} occupies the tetrahedral sites at (1/8, 1/8, 1/8) and both $Fe^{2+}$and Fe^{3+} occupy the octahedral sites at (1/2, 1/2, 1/2) with sulfur atoms at (u, u, u) positions (Figure 3). The values of u from the refinements are found to be independent of temperature: the D1B data yield the value u = 0.2550(2), while the D1A data give u = 0.2542(2). The lattice parameter a_0 smoothly increases with temperature, following the expected thermal expansion. This is a feature of the enharmonic terms in the interatomic potentials; a_0 values for particular temperatures are listed in Table 1. The small systematic difference between the a_0 values refined from the D1A and D1B data is probably due to small uncertainties in the wavelength calibrations.

[9] The magnetic refinement confirms a collinear ferrimagnetic structure (magnetic space group F-1) (Figure 3), in which the iron moments on the tetrahedral and octahedral sites are antiparallel. The values of the magnetic moments M_A and M_B of the two Fe sites are tabulated in Table 1 for specific temperatures, along with the net magnetic moment per formula unit $|2\ M_B + M_A|$. The temperature dependence of the magnitude of the moments is shown in Figure 4 (where the scale for the net magnetic moment has been shifted for clarity (right-hand axis)). Agreement between the D1A and D1B refinements is generally excellent, although there is a systematic difference of about 0.2 Bohr magneton (μ_B) between the values for the tetrahedral site moments; that is, at room temperature the D1B data give M_A = 3.20(7) μ_B, while for the D1A data M_A = 2.97(8) μ_B. The origin of this discrepancy is not clear, but it may be related to correlations with thermal parameters in the fits. That is, thermal vibrations change the scattering amplitude by the Debye-Waller factor, which drops off with increasing 2θ, as does the magnetic scattering amplitude magnetic form factor, so it is possible that there would be correlations between the magnetic moments M and the thermal parameters. Nevertheless, the agreement between the two data sets for the octahedral site moments is excellent. There are several qualitative features common to both data sets. First, the magnitude of the moments at both Fe sites is similar (~3.0 μ_B at room temperature); these values are much smaller than those found in magnetite [e.g., *Klotz et al.*, 2006]. Second, the magnetic moment per formula unit is 3.0 μ_B at room temperature, rising to ~3.4 μ_B at 10 K; these values are in good agreement with bulk magnetic measurements which give M_s ~59 A m^2 kg^{-1} (3.12 μ_B fu^{-1}) at room temperature and M_s ~64 A m^2 kg^{-1} (3.39 μ_B fu^{-1}) at 10 K [*Chang et al.*, 2008]. Third, while the B site moment increases as temperature decreases, reaching 3.25 μ_B at 10 K, the A site moment is practically independent of temperature. The temperature dependence of the sublattice magnetizations

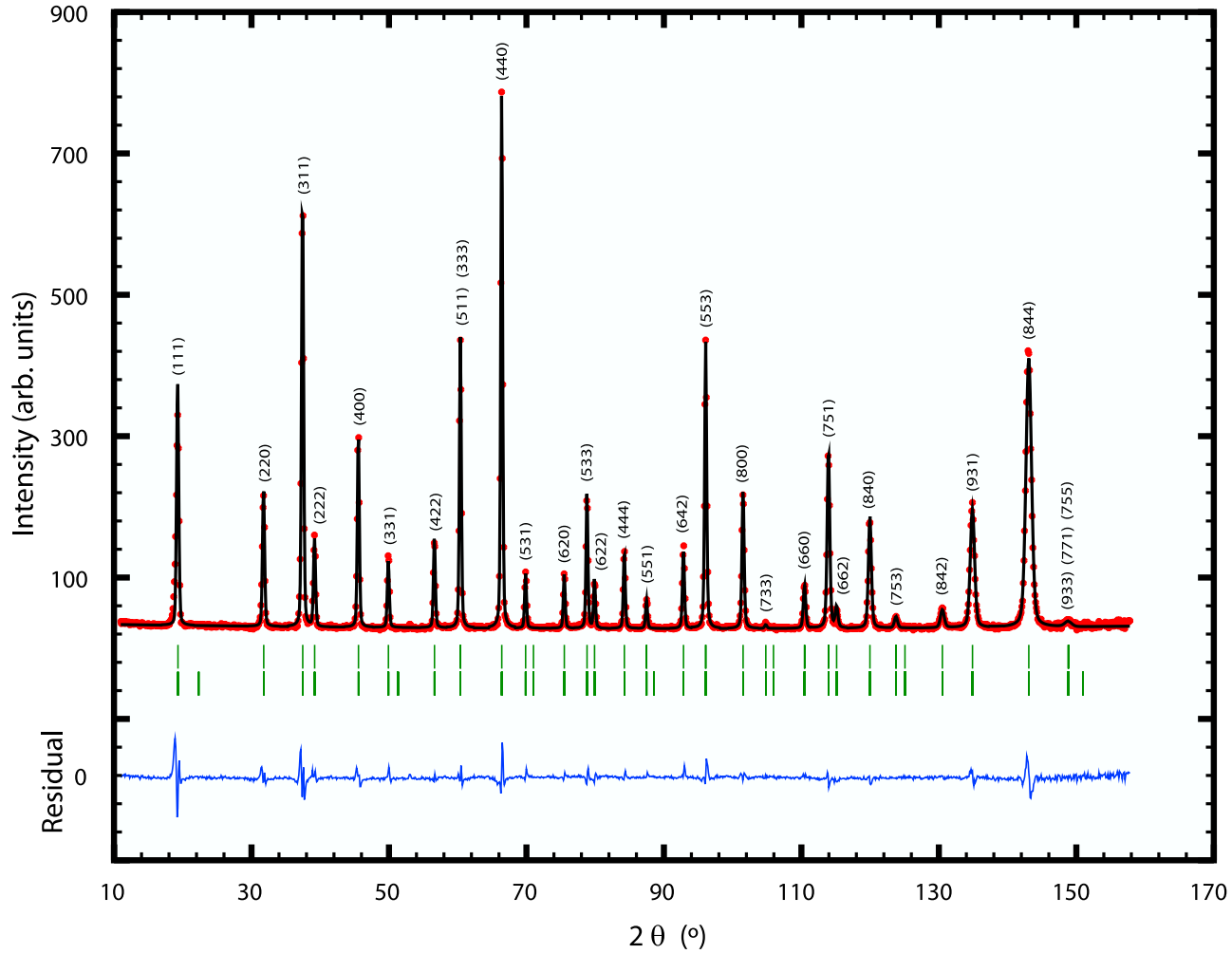

Figure 2. Rietveld refinement of the high-resolution NPD pattern for the synthetic greigite sample recorded on the D1A neutron powder diffractometer (λ = 1.91 Å) at 200 K. The observed and calculated intensities are shown by red dots and by a black solid line, respectively. The blue line is the calculated residual between experimentally measured values and the refinement. Green tick marks indicate the positions of the nuclear (top curves) and magnetic (bottom curves) Bragg reflections. The model enables refinement of both the positional parameter and the magnetic moments of the two sublattices.

for greigite resembles those of R-type ferrimagnets, as found in many ferrites, e.g., $NiFe_2O_4$. By contrast, magnetite is a Q-type ferrimagnet, in which both sublattice magnetizations behave like true ferromagnets. Greigite has a much weaker *A-B* exchange interaction than magnetite [*Chang et al.*, 2008], which might explain the different sublattice magnetization curves for greigite and magnetite.

[10] There were no significant differences in the qualities of the refinements of the D1A patterns at 10, 100, 200, and 290 K or in the D1B temperature scan from 290 K to 10 K. This is consistent with previous studies of greigite in which no evidence has been found for an equivalent of the Verwey transition in magnetite or for any other magnetic transition [*Spender et al.*, 1972; *Moskowitz et al.*, 1993; *Roberts*, 1995; *Chang et al.*, 2007, 2008].

[11] In the spinel structure, the sulfur coordinate u is related to the Fe-S bond lengths d_A and d_B at the A and B sites by $d_A = \sqrt{3}\, a(u - 1/8)$ and $d_B = a(1/2 - u)$. From the fit parameters, we find d_A = 2.21(1) Å and d_B = 2.42(1) Å. These values are somewhat larger than those for the Fe-O bond lengths in magnetite (d_A = 1.90 Å and d_B = 2.05 Å [*Klotz et al.*, 2006]), as would be expected for a larger ligand ionic radius. The ratio d_B/d_A is 1.078 for magnetite but is 1.093 for greigite: this may indicate a greater mixed valent character for the octahedral sites of greigite compared to magnetite.

3.2. Polarized Neutron Diffractometry

[12] Polarized neutron diffraction was carried out to confirm the magnetic structure of greigite. Greigite is unstable at high temperature and decomposes before reaching its Curie temperature T_C [e.g., *Krs et al.*, 1992; *Roberts*, 1995; *Dekkers et al.*, 2000; *Chang et al.*, 2008]. It is therefore not possible to measure neutron diffraction patterns above and below T_C in order to separate the magnetic component of the Bragg peaks. Instead, we used polarized neutrons with a vertical applied field to saturate the magnetization of the sample normal to the scattering plane. This enabled isothermal separation of the nuclear and magnetic scattering. For a collinear ferromagnet or ferrimagnet, the

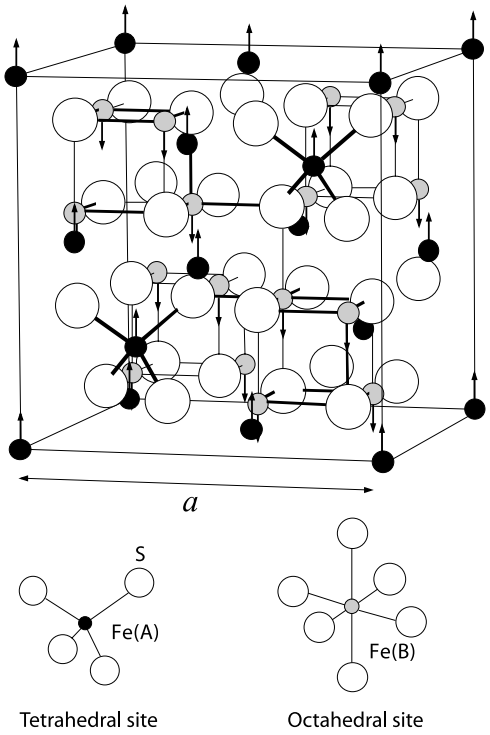

Figure 3. Crystallographic and magnetic structure of Fe_3S_4 determined from NPD and polarized neutron diffraction (adapted from *García and Subías* [2004], copyright Institute of Physics). Greigite crystallizes in the inverse spinel structure with a cubic close-packed sulfur array (space group $Fd\bar{3}$ m, Z = 8). Fe^{3+} occupies the *A* (tetrahedral) sites, while both $Fe^{2+}$and Fe^{3+} occupy the *B* (octahedral) sites. A collinear ferrimagnetic spin arrangement was found in greigite with antiferromagnetic coupling between the octahedral and tetrahedral Fe ions. The lattice parameter is *a*. The arrows represent the magnetic moment directions of each Fe ion. Magnetic moments are shown to be aligned along the crystallographic *c* axis because the easy axis of magnetization is the [100] crystallographic axis [*Yamaguchi and Wada*, 1970]. The absolute moment directions within the unit cell cannot be obtained because for the cubic phase, only relative orientations of moments affect the NPD intensities.

flipping ratios for the saturated state give a measure of the ratio of the magnetic to nuclear structure factors. The nonspin-flip scattering intensities can be described by the interference of the nuclear and magnetic scattering [*Brown and Forsyth*, 1964]:

$$I(\pm,\pm) = C\left|F_N \pm F_{mag}\right|^2, \tag{1}$$

where F_N and F_{mag} are the nuclear and magnetic structure factors and C is a constant. The ideal flipping ratio R is defined as the ratio between the diffraction intensities of neutrons with spin-up and spin-down [*Brown and Forsyth*, 1964]:

$$R = \frac{I(+,+)}{I(-,-)} = \frac{(F_N + F_M)^2}{(F_N - F_M)^2} = \frac{(1+\gamma)^2}{(1-\gamma)^2}, \tag{2}$$

where $\gamma = F_N/F_M$ is the ratio of nuclear to magnetic structure factors. The flipping ratio R is determined by measuring the diffracted intensities with the neutron spin flipper turned alternately on and off. In practice, the measured flipping ratio differs from the ideal value because (1) the incident beam is not 100% polarized, (2) the neutron spin flipper is not 100% efficient, and (3) the sample may introduce a degree of beam depolarization. When these factors are taken into account, the corrected flipping ratio becomes [*Brown and Forsyth*, 1964]

$$R = \frac{1 + \gamma^2 + 2PD\gamma}{1 + \gamma^2 - 2\eta PD\gamma}, \tag{3}$$

where P is the initial beam polarization, η is the flipping efficiency, and D is the depolarization correction factor.

[13] Diffraction profiles of the nonspin-flip intensities (I (+, +) and I (−, −)) at room temperature in a 5 T magnetic field are shown in Figure 5a. In addition to greigite reflections, two strong Bragg peaks (at ∼83° and 100° 2θ) can be attributed to the (111) and (200) Bragg peaks from the aluminum sample can (Figure 5a). Aluminum is not magnetic, so the spin-up and spin-down neutron scattering have the same intensities. For greigite, the Bragg peak intensities for spin-up are mostly greater than those for spin-down (i.e., the flipping ratio R is greater than one) (Figure 5a). There are two exceptions: for both the (220)

Table 1. Structural Parameters for Greigite From FULLPROF Rietveld Refinements[a]

		Temperature (K)			
Instrument	Parameter	10	100	200	290
D1B	M_A (μ_B)	3.16 ± 0.07	3.20 ± 0.07	3.19 ± 0.07	3.20 ± 0.07
D1B	M_B (μ_B)	−3.24 ± 0.05	−3.19 ± 0.05	−3.16 ± 0.05	−3.08 ± 0.05
D1B	M fu^{-1} (μ_B)	3.32 ± 0.09	3.18 ± 0.09	3.13 ± 0.09	2.96 ± 0.09
D1B	a_0 (Å)	9.8559(3)	9.8585(3)	9.8650(3)	9.8734(3)
D1B	u	0.2552(7)	0.2549(8)	0.2552(8)	0.2552(8)
D1A	M_A (μ_B)	3.00 ± 0.08	2.99 ± 0.08	3.01 ± 0.08	2.97 ± 0.08
D1A	M_B (μ_B)	−3.26 ± 0.06	−3.17 ± 0.06	−3.07 ± 0.06	−3.00 ± 0.06
D1A	M fu^{-1} (μ_B)	3.52 ± 0.10	3.35 ± 0.10	3.13 ± 0.10	3.03 ± 0.10
D1A	a_0 (Å)	9.8538(2)	9.8552(2)	9.8645(2)	9.8718(2)
D1A	u	0.2542(7)	0.2541(6)	0.2546(4)	0.2540(6)

[a] M_A and M_B are the magnetic moments of the *A* and *B* sites, respectively, M fu^{-1} is the total magnetic moment per formula, unit a_0 is the lattice parameter, and u is the internal sulfur coordinate. Values in parentheses are standard deviations.

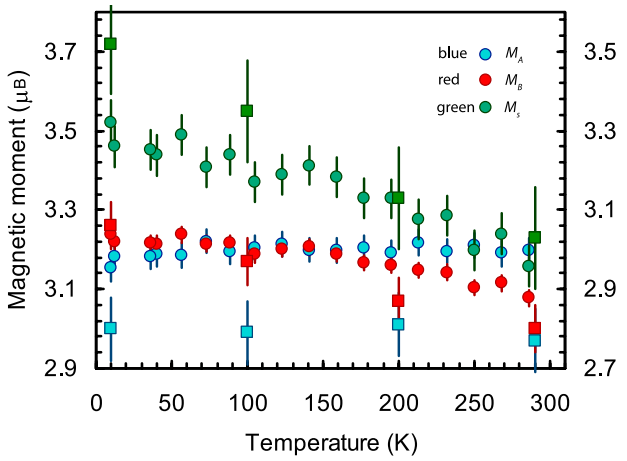

Figure 4. Temperature dependence of the sublattice (M_A and M_B) and total spontaneous (M_s) magnetizations for greigite. The blue and red circles are the sublattice moments of the tetrahedral sites M_A and octahedral sites M_B, respectively, derived from analysis of the D1B data. The blue and red squares are M_A and M_B values refined from the D1A data. The green circles and squares correspond to the moment per formula unit M fu^{-1} = (2 M_B − M_A) derived from the D1B and D1A data, respectively. For clarity, the scale of the M fu^{-1} data has been shifted as shown on the right-hand axis. The D1B data are averaged over five temperature points to reduce scatter. The average magnetic moment of the Fe ions on the B sites decreases with increasing temperature, while the A site moments appear to be temperature-independent below room temperature, which indicates that greigite is probably an R-type ferrimagnet.

and (422) reflections, the spin-down intensity is greater than the spin-up intensity (flipping ratio less than one). This may be seen more clearly in Figure 5b, where the difference between the spin-up and spin-down patterns is plotted: here, the (220) and (422) reflections appear as negative peaks. The difference pattern is proportional to $4F_NF_M$, the product of the nuclear and magnetic structure factors. For the (220) reflection, the nuclear structure factor is $F_N = -8b_{Fe}$ (with a negligibly small sulfur contribution) while the magnetic structure factor is $F_M = -8p_A$. Here, b_{Fe} is the nuclear scattering amplitude of iron, while p_A is the magnetic scattering amplitude for the tetrahedral Fe site:

$$p_A = 2.69 \times 10^{-15}\mu_A f(Q), \qquad (4)$$

where μ_A is the Fe moment on the tetrahedral sites and $f(Q)$ is the iron 3d form factor. The negative value of the product F_NF_M for the (220) reflection means, therefore, that μ_A is antiparallel to the net magnetization. For the (422) reflection, the structure factors are $F_N = 8b_{Fe}$ and $F_M = 8p_A$, so the same argument applies as for the (220) reflection. This gives direct support to the collinear ferrimagnetic model of greigite in which the tetrahedral and octahedral Fe ions are antiferromagnetically coupled. For this model, it is readily shown that the nuclear and magnetic structure factors have the same sign as for all the other peaks, so that we expect flipping ratios greater than unity, as observed.

[14] To enable quantitative comparison of the D7 data with the magnetic structure of greigite, we compare in Table 2 the flipping ratios (R_{exp}) for the 10 Bragg peaks measured at 20 K with the flipping ratios (R_{calc}) calculated from the magnetic and nuclear structure factors using the 10 K D1A data (i.e., sublattice moments and structural parameters). The R_{calc} data correspond to the ideal flipping ratio values, as defined in equation (2). Large discrepancies between R_{exp} and R_{calc} are evident for the reflections with γ values ($\gamma = F_N/F_M$) close to unity. Corrections for neutron polarization P, depolarization D, and flipping efficiency η are especially important. Values for P and η expected from the supermirror polarizers and spin flipper on D7 are normally about 0.9. For a bulk single crystal, the depolarization factor D is usually close to unity, but the values depend on the sample geometry and degree of magnetic saturation [*Brown and Forsyth*, 1964]. However, the present sample is a fine powder and the degree of beam depolarization will be expected to be relatively high, because of the large contrast in B field within and between individual grains. The best fit between R_{exp} and R_{calc} is obtained with PD = 0.7 and η = 0.9. With these values, the corrected flipping ratio (Table 2) agrees well with measured values (R_{exp}) within the error bars in all cases, except for the (422) reflection, which is contaminated by the strong aluminum (200) Bragg peak. We conclude that the D7 polarized neutron data confirm the magnetic structure of greigite derived from Rietveld analysis of unpolarized neutron

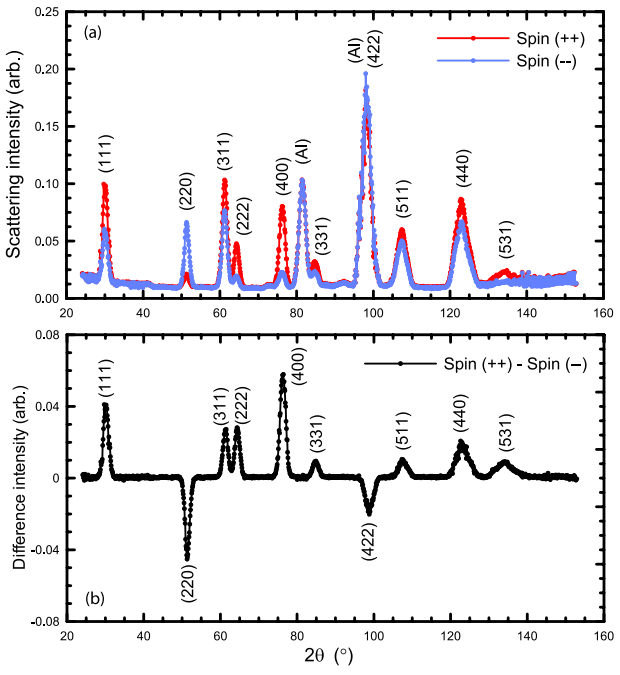

Figure 5. Spin-polarized neutron diffraction patterns for the synthetic greigite sample at room temperature in a magnetic field of 5 T. (a) Neutron spin-up (red curve) and spin-down (blue curve) diffraction patterns. Note the overlap of the greigite (422) reflection with the strong aluminum (200) peak. (b) Difference between the patterns shown in Figure 5a (spin-up minus spin-down patterns).

Table 2. Flipping Ratios for Polarized Neutron Diffraction for Greigite at 20 K[a]

(*hkl*)	$R_{exp} = I^{++}/I^{-}$	ΔR_{exp}	R_{calc}	Corrected R_{calc}
(111)	1.90	0.11	2.643	1.87
(220)	0.20	0.03	0.027	0.21
(311)	1.45	0.05	1.766	1.45
(222)	3.36	0.34	13.20	3.50
(400)	4.52	0.23	190.0	4.50
(331)	1.61	0.11	2.366	1.66
(422)[b]	0.85	0.02	0.097	0.28
(511) and (333)	1.22	0.04	1.471	1.29
(440)	1.37	0.05	1.583	1.35
(531)	2.81	0.44	7.276	3.00

[a]The experimental flipping ratio R_{exp} compared to R_{calc} calculated from the structure factors from the fit to the 10 K D1A data. The corrected R_{calc} values are corrected by the factor $PD = 0.7$ and a flipping efficiency $\eta = 0.9$. These values agree well with R_{exp} except in the case of the (422) reflection.
[b]Overlaps with the strong (200) peak for aluminum.

diffraction data. One would normally expect polarized neutron diffractometry to give higher quality information than unpolarized data. This is the case for bulk single crystals; however, for powder samples the depolarization corrections can be large and it is difficult to determine these independently.

4. Discussion

4.1. Magnetic Structure of Greigite

[15] NPD and polarized neutron diffraction experiments have enabled unambiguous assignment of the magnetic structure of greigite for the first time, confirming a collinear ferrimagnetic structure in which the iron moments on the tetrahedral sites are antiparallel to those on the octahedral sites. There is no evidence for significant spin canting in greigite from analysis of our neutron diffraction pattern because there are no extra peaks in the neutron diffraction pattern. This is also supported by the fact that there is no difference between the zero field neutron diffraction pattern and that measured in a 5 T field. In-field Mössbauer measurements also support the absence of significant spin canting in greigite [*Chang et al.*, 2008]. *Letard et al.* [2005] proposed greigite to be a lacunary iron sulfide based on the differences between the observed X-ray magnetic circular dichroism (XMCD) spectra of greigite and magnetite. *Rickard and Luther* [2007] also argued that the composition of greigite is still not well constrained and that greigite probably displays some degree of nonstoichiometry. Mössbauer measurements give possible evidence for nonstoichiometry of greigite [*Coey et al.*, 1970; *Spender et al.*, 1972]. However, *Qian et al.* [1999] determined by spectrophotometric analysis that the composition of greigite in synthetic samples was $Fe_{2.994}S_4$, which is nearly stoichiometric. Our Rietveld profile analysis of the neutron diffraction data included parameters for partial occupancy of the Fe sites. However, no departure from stoichiometry was found in the parameters for the fitted profiles. The quality of the fits indicates that our synthetic sample does not have a significant vacancy concentration. In the standard inverse spinel structure, Fe^{3+} occupies the tetrahedral sites, while both Fe^{2+} and Fe^{3+} occupy the octahedral sites. Considering the ionic model, the formula of greigite can then be written as $[\uparrow Fe^{3+}]^A$ $[\downarrow Fe^{2+}$ $\downarrow Fe^{3+}]^B$ S_4^{2-}. In the *Néel* [1948] model for magnetite, the ions have their localized spin-only moment, leading to sublattice Fe moments of 5 μ_B for the tetrahedral *A* sites and 4.5 μ_B for the octahedral *B* sites and a moment per formula unit of 4 μ_B. For magnetite, while the net magnetization is correctly predicted by this model, the sublattice moments are not: neutron diffraction measurements give $M_A = 4.2$ μ_B, $M_B = 3.97$ μ_B at 130 K [*Wright et al.*, 2002] and $M_A = 4.05$ μ_B, $M_B = 3.60$ μ_B at 300 K [*Klotz et al.*, 2006]. This suggests that there is a degree of delocalization of the *d* electrons in magnetite. Band calculations [e.g., *Zhang and Satpathy*, 1991] indicate that magnetite is a semimetal where the Fermi level intersects the minority spin $3d$ t_{2g} bands of the Fe atoms on the octahedral sites. More recent calculations [*Szotek et al.*, 2006] are based on the self-interaction corrected local spin density approximation, which gives a better account of electron correlations than other methods. They find that the lowest energy solution is ferrimagnetic with Fe^{3+} on both tetrahedral and octahedral sites, due to a delocalization of the sixth *d* electron of the original Fe^{2+} ions. The calculated sublattice moments are $M_A = 4.02$ μ_B and $M_B = 3.90$ μ_B, which is close to the measured values.

[16] The sublattice moments in greigite have similar magnitudes to each other, as in magnetite, and are even further removed from the localized model of *Néel* [1948], which suggests a higher degree of delocalization of the *d* electrons. The electronic structure of greigite, i.e., the valence state of iron, is still not clear. No band structure calculations are available for greigite so far, although spin-polarized multiple scattering calculations have been reported for Fe-S clusters [*Braga et al.*, 1988]. Their value for the moment per formula unit is 3.02 μ_B, which is close to the experimental value, but this agreement appears to be fortuitous because the *A* and *B* site moments were estimated to be 2.0 μ_B and 2.5 μ_B, respectively.

[17] The magnetic structure model for greigite is consistent with Mössbauer spectroscopic measurements. The hyperfine fields for the *A* and *B* sites are −31.9 and −32.7 T, respectively, at 4 K, while at room temperature they are almost identical (−31.2 T, −31.5 T) [*Chang et al.*, 2008]. This is in qualitative accord with the sublattice moments and their temperature dependence. The values of isomer shifts for greigite indicate that iron at the *A* sites is predominantly ferric, while the *B* sites are occupied by both ferrous and ferric ions if fast electronic hopping between

them occurs [e.g., *Coey et al.*, 1970; *Spender et al.*, 1972; *Vandenberghe et al.*, 1992; *Chang et al.*, 2008]. Application of a large magnetic field splits the Mössbauer spectra for greigite, with the hyperfine field at *A* sites increasing and that at *B* sites decreasing. The $\Delta M = 0$ transitions disappear at high fields, which is as expected if the magnetic moments are parallel or antiparallel to the applied field. These observations are consistent with a collinear ferrimagnetic structure.

[18] XMCD spectra for greigite contain only two distinct absorption peaks, which so far have been attributed to the *B* site Fe^{2+} and *B* site Fe^{3+}, while the *A* site absorption peak is not clear [*Letard et al.*, 2005; L. Chang et al., unpublished experimental data, 2007]. Further analysis of such data appears to be necessary.

4.2. Origin of Lower Magnetic Moments in Greigite Compared to Magnetite

[19] As obtained from high-resolution NPD patterns, the spontaneous magnetization M_s for greigite at room temperature is $\sim$3.0 μ_B fu^{-1}, which is slightly lower than the value of $\sim$59 A m^2 kg^{-1} (3.13 μ_B fu^{-1}) obtained from a superconducting quantum interference device (SQUID) magnetometer on bulk samples [*Chang et al.*, 2008]. A similar contrast in results from different techniques has been observed for magnetite [e.g., *Wright et al.*, 2002]. This slight deviation for magnetite has been attributed to the residual orbital moments [e.g., *Néel*, 1948; *Walz*, 2002]. It must be kept in mind that the sublattice moments measured by neutron diffraction correspond to the 3*d* component of the magnetization density: any spin transfer to the ligands (due to covalency or delocalization) would not be readily detected by neutrons because the magnetic form factor of the ligands drops rapidly with increasing wave vector.

[20] The apparently low M_s values for greigite in the literature (normally less than one third that of magnetite) are not an intrinsic property of greigite because previously reported greigite samples were not pure and also had small particle size, leading to large SP fractions, as argued by *Dekkers et al.* [2000] and *Chang et al.* [2008]. The synthetic greigite samples analyzed in this study have been confirmed by a range of analyses to be virtually pure. Therefore, the measured M_s from these samples represents the most accurate published value for greigite [*Chang et al.*, 2008]. Surface magnetic effects may contribute to low M_s in fine particle systems. It is well known that spins in the surface layer can be inclined at various angles to the direction of net moment, as observed in many systems containing ultrafine magnetic particles, e.g., γ-Fe_2O_3 [e.g., *Coey*, 1971] and $NiFe_2O_4$ [*Kodama et al.*, 1996]. Unlike most of the synthetic greigite samples with significant SP behavior reported in the literature [e.g., *Uda*, 1965; *Spender et al.*, 1972; *Dekkers et al.*, 2000], our samples have much larger grain sizes (tens of microns) with only small concentrations of extremely fine particles [*Chang et al.*, 2008]. There may be surface magnetic effects in our finest greigite grains, but their contributions can be ignored. Therefore, they should not cause a significant decrease of M_s in our synthetic greigite samples. The presence of vacancies can also lower M_s. For example, maghemite (γ-Fe_2O_3) has a similar inverse spinel structure as magnetite except that one sixth of the *B* sites are occupied by vacancies ($[\uparrow Fe^{3+}]^A$ $[\downarrow Fe^{3+}_{5/3}\ \square_{1/3}]^B$ O_4^{2-}), which results in a lower M_s compared to magnetite. However, neutron scattering results indicate that there is no significant vacancy concentration in our greigite sample. Our overall conclusion is that the average magnetic moment for greigite is lower than for magnetite, but it is not as low as was previously thought. It is, therefore, necessary to explain why greigite has a lower spontaneous magnetization than magnetite.

[21] The difference in M_s between magnetite and greigite probably relates to different degrees of covalency between Fe ions with oxygen and sulfur ligands, respectively, although greigite is considered to be the most ionic thiospinel. Increased covalency reduces the ionicity of the ions, which makes the ligands (O or S) less negative and the Fe cations less positive. Normally, covalency would be stronger with sulfur ligands than with oxygen because there should be more overlap of wave function between Fe and S ions (a larger covalency radius) compared to Fe and O ions. This increased covalency effect is also suggested by the lower hyperfine fields for greigite than for magnetite [e.g., *Morice et al.*, 1969; *Coey et al.*, 1970; *Spender et al.*, 1972; *Vandenberghe et al.*, 1992; *Chang et al.*, 2008] and decreased separation between the absorption peaks for the Fe^{2+} and Fe^{3+} in octahedral sites in the XMCD spectra of greigite [*Letard et al.*, 2005; Chang et al., unpublished experimental data, 2007]. From a band point of view, we can equate increased covalency with a higher degree of overlap and hybridization between the sulfur 3*p* and iron 3*d* bands. Neutron diffraction results for Fe_3Se_4, which has a defect NiAs structure, also indicate lower magnetic moments of the iron ions [*Andresen*, 1968]. This is probably explained by a further increased covalency with selenium ligands. *Coey et al.* [1970] carried out conductivity measurements on synthetic greigite samples and showed that the resistivity was in the range of 10^{-1}–10^{-3} Ω cm. They concluded that there is some electron delocalization in greigite, which is probably a result of cation-anion covalence because the *B*-*B* cation distance (3.49 Å) is probably too large for direct cation-cation overlap [*Coey et al.*, 1970]. The increased delocalization of electrons in greigite would effectively lower the ordered moment. We therefore conclude that the lower spontaneous magnetization of greigite compared to magnetite results from increased covalency between Fe and S ligands compared to O ligands, or from greater delocalization of the 3*d* electrons in greigite.

4.3. Absence of Low-Temperature Structural Changes in Greigite

[22] We cannot claim from our NPD and polarized neutron diffraction results to have demonstrated that greigite has no low-temperature equivalent to the Verwey transition because the crystallographic changes found at the Verwey transition in magnetite are subtle, and difficult to resolve [*Wright et al.*, 2001, 2002]. However, the smooth variation of our fitted parameters from room temperature to low temperature are consistent with other measurements that indicate that greigite has no low-temperature phase transition [*Coey et al.*, 1970; *Spender et al.*, 1972; *Vandenberghe et al.*, 1992; *Moskowitz et al.*, 1993; *Roberts*, 1995; *Chang et al.*, 2007, 2008]. It is not possible to explain the absence of a low-temperature phase transition in greigite at the moment, given that the mechanism for the Verwey transi-

tion is not yet fully understood. Regardless, we assume that the replacement of oxygen by sulfur in greigite has suppressed any analog to the Verwey transition in greigite.

5. Conclusions

[23] NPD and polarized neutron diffraction experiments on pure synthetic greigite enable us to provide the first determination of its magnetic structure. These data provide a direct measure of the intrinsic magnetism of greigite. Our results confirm that greigite has a collinear ferrimagnetic structure, similar to the magnetic structure of magnetite above the Verwey transition. Our analysis of our neutron diffraction patterns indicates that greigite does not have a significant vacancy concentration and there is also no evidence of significant spin canting in greigite. The average magnetic moments of Fe ions for both the *A* and *B* sublattices at room temperature, refined from high-resolution NPD measurements, are $\sim$3.0 μ_B with M_s of 3.0 μ_B fu^{-1}. At 10 K, the *A* site moment is 3.08 μ_B, while the *B* site moment is 3.25 μ_B with M_s of 3.4 μ_B fu^{-1}. The average magnetic moment of the Fe ions at the *B* sites decreases with increasing temperature, while the *A* site moments vary little up to room temperature. This indicates that greigite is an R-type ferrimagnet, which is consistent with the measured lower *A-B* exchange interaction for greigite than magnetite. Neutron diffraction and magnetic measurements consistently indicate lower magnetic moments in greigite compared to magnetite. It is likely that the low magnetic moments in greigite arise from a higher degree of covalency between Fe ions and the sulfur ligands, or from greater delocalization of the 3*d* electrons. A band structure calculation for greigite is long overdue. No low-temperature crystal or magnetic structure change is evident for greigite in either the high-resolution NPD or the polarized neutron diffraction; this is consistent with other published data that demonstrate the lack of a low-temperature phase transition in greigite.

[24] **Acknowledgments.** Liao Chang is supported by a Dorothy Hodgkin Postgraduate Award, funded by Hutchison Whampoa Limited and the U.K. Natural Environment Research Council. Greigite synthesis was supported by the National Natural Science Foundation of China under grants 20321101, 20125103, and 90206034. Access to beam time was supported by the Institut Laue-Langevin. We thank G. van der Laan and S. K. Banerjee for helpful discussions and M. Dekkers and an anonymous reviewer for comments that improved the manuscript.

References

Andresen, A. F. (1968), A neutron diffraction investigation of Fe_3Se_4, *Acta Chem. Scand.*, *22*, 827–835, doi:10.3891/acta.chem.scand.22-0827.

Berner, R. A. (1984), Sedimentary pyrite formation: An update, *Geochim. Cosmochim. Acta*, *48*, 605–615, doi:10.1016/0016-7037(84)90089-9.

Braga, M., S. K. Lie, C. A. Taft, and W. A. Lester Jr. (1988), Electronic structure, hyperfine interactions, and magnetic properties for iron octahedral sulfides, *Phys. Rev.*, *38*, 10,837–10,851.

Brown, P. J., and J. B. Forsyth (1964), The determination of beam polarization and flipping efficiency in polarized neutron diffractometry, *Br. J. Appl. Phys.*, *15*, 1529–1533, doi:10.1088/0508-3443/15/12/313.

Chang, L., A. P. Roberts, A. R. Muxworthy, Y. Tang, Q. Chen, C. J. Rowan, Q. Liu, and P. Pruner (2007), Magnetic characteristics of synthetic pseudo-single-domain and multi-domain greigite (Fe_3S_4), *Geophys. Res. Lett.*, *34*, L24304, doi:10.1029/2007GL032114.

Chang, L., A. P. Roberts, Y. Tang, B. D. Rainford, A. R. Muxworthy, and Q. Chen (2008), Fundamental magnetic parameters from pure synthetic greigite (Fe_3S_4), *J. Geophys. Res.*, *113*, B06104, doi:10.1029/2007JB005502.

Chen, X. Y., X. F. Zhang, J. X. Wan, Z. H. Wang, and Y. T. Qian (2005), Selective fabrication of metastable greigite (Fe_3S_4) nanocrystallites and its magnetic properties through a simple solution-based route, *Chem. Phys. Lett.*, *403*, 396–399, doi:10.1016/j.cplett.2005.01.050.

Coey, J. M. D. (1971), Non-collinear spin arrangement in ultrafine ferrimagnetic crystallites, *Phys. Rev. Lett.*, *27*, 1140–1142, doi:10.1103/PhysRevLett.27.1140.

Coey, J. M. D., M. R. Spender, and A. H. Morrish (1970), The magnetic structure of the spinel, Fe_3S_4, *Solid State Commun.*, *8*, 1605–1608, doi:10.1016/0038-1098(70)90473-4.

Dekkers, M. J., and M. A. A. Schoonen (1996), Magnetic properties of hydrothermally synthesized greigite-I. Rock magnetic parameters at room temperature, *Geophys. J. Int.*, *126*, 360–368, doi:10.1111/j.1365-246X.1996.tb05296.x.

Dekkers, M. J., H. F. Passier, and M. A. A. Schoonen (2000), Magnetic properties of hydrothermally synthesized greigite-II. High- and low-temperature characteristics, *Geophys. J. Int.*, *141*, 809–819, doi:10.1046/j.1365-246x.2000.00129.x.

Farina, M., D. M. S. Esquivel, and H. G. P. Lins de Barros (1990), Magnetic iron-sulphur crystals from a magnetotactic microorganism, *Nature*, *343*, 256–258, doi:10.1038/343256a0.

García, J., and G. Subías (2004), The Verwey transition—A new perspective, *J. Phys. Condens. Matter*, *16*, R145–R178, doi:10.1088/0953-8984/16/7/R01.

Goodenough, J. B., and G. A. Fatseas (1982), Mössbauer ^{57}Fe isomer shift as a measure of valence in mixed-valence iron sulfides, *J. Solid State Chem.*, *41*, 1–22, doi:10.1016/0022-4596(82)90028-7.

He, Z. B., S. H. Yu, X. Y. Zhou, X. G. Li, and J. F. Qu (2006), Magnetic-field-induced phase-selective synthesis of ferrosulfide microrods by a hydrothermal process: Microstructure control and magnetic properties, *Adv. Funct. Mater.*, *16*, 1105–1111, doi:10.1002/adfm.200500580.

Hoffmann, V. (1992), Greigite (Fe_3S_4): Magnetic properties and first domain observations, *Phys. Earth Planet. Inter.*, *70*, 288–301, doi:10.1016/0031-9201(92)90195-2.

Jiang, W. T., C. S. Horng, A. P. Roberts, and D. R. Peacor (2001), Contradictory magnetic polarities in sediments and variable timing of neoformation of authigenic greigite, *Earth Planet. Sci. Lett.*, *193*, 1–12, doi:10.1016/S0012-821X(01)00497-6.

Klotz, S., G. Rousse, T. Strässle, C. L. Bull, and M. Guthrie (2006), Nuclear and magnetic structure of magnetite under pressure to 5.3 GPa and low temperatures to 130 K by neutron scattering, *Phys. Rev. B*, *74*, 012410, doi:10.1103/PhysRevB.74.012410.

Kodama, R. H., A. E. Berkowitz, E. J. McNiff Jr., and S. Foner (1996), Surface spin disorder in $NiFe_2O_4$ nanoparticles, *Phys. Rev. Lett.*, *77*, 394–397, doi:10.1103/PhysRevLett.77.394.

Krs, M., F. Novák, M. Krsová, P. Pruner, L. Koulíková, and J. Jansa (1992), Magnetic properties and metastability of greigite-smythite mineralization in brown-coal basins of the Krusné Hory Piedmont, Bohemia, *Phys. Earth Planet. Inter.*, *70*, 273–287, doi:10.1016/0031-9201(92)90194-Z.

Letard, I., P. Sainctavit, N. Menguy, J.-P. Valet, A. Isambert, M. Dekkers, and A. Gloter (2005), Mineralogy of greigite Fe_3S_4, *Phys. Scr.*, *T115*, 489–491, doi:10.1238/Physica.Topical.115a00489.

Mann, S., N. H. C. Sparks, R. B. Frankel, D. A. Bazylinski, and H. W. Jannasch (1990), Biomineralization of ferrimagnetic greigite (Fe_3S_4) and iron pyrite (FeS_2) in a magnetotactic bacterium, *Nature*, *343*, 258–261, doi:10.1038/343258a0.

Moon, R. M., T. Riste, and W. C. Koehler (1969), Polarization analysis of thermal-neutron scattering, *Phys. Rev.*, *181*, 920–931, doi:10.1103/PhysRev.181.920.

Morice, J. A., L. V. C. Rees, and D. T. Rickard (1969), Mössbauer studies of iron sulphides, *J. Inorg. Nucl. Chem.*, *31*, 3797–3802, doi:10.1016/0022-1902(69)80299-X.

Moskowitz, B. M., R. B. Frankel, and D. A. Bazylinski (1993), Rock magnetic criteria for the detection of biogenic magnetite, *Earth Planet. Sci. Lett.*, *120*, 283–300, doi:10.1016/0012-821X(93)90245-5.

Néel, L. (1948), Propriétés magnétiques des ferrites: Ferrimagnétisme et antiferromagnétisme, *Ann. Phys.*, *3*, 137–198.

Qian, X. F., X. M. Zhang, C. Wang, Y. Xie, W. Z. Wang, and Y. T. Qian (1999), The preparation and phase transition of nanocrystalline iron sulfides via toluene-thermal process, *Mater. Sci. Eng.*, *64*, 170–173, doi:10.1016/S0921-5107(99)00145-2.

Reynolds, R. L., M. L. Tuttle, C. A. Rice, N. S. Fishman, J. A. Karachewski, and D. M. Sherman (1994), Magnetization and geochemistry of greigite-bearing Cretaceous strata, North Slope, Alaska, *Am. J. Sci.*, *294*, 485–528.

Rickard, D., and G. W. Luther III (2007), Chemistry of iron sulfides, *Chem. Rev.*, *107*, 514–562, doi:10.1021/cr0503658.

Roberts, A. P. (1995), Magnetic properties of sedimentary greigite (Fe_3S_4), *Earth Planet. Sci. Lett.*, *134*, 227–236, doi:10.1016/0012-821X(95)00131-U.

Roberts, A. P., and R. Weaver (2005), Multiple mechanisms of remagnetization involving sedimentary greigite (Fe_3S_4), *Earth Planet. Sci. Lett.*, *231*, 263–277, doi:10.1016/j.epsl.2004.11.024.

Rodríguez-Carvajal, J. (1993), Recent advances in magnetic structure determination by neutron powder diffraction, *Physica B*, *192*, 55–69, doi:10.1016/0921-4526(93)90108-I.

Sherman, D. M. (1990), Mössbauer spectra, crystal chemistry, and electronic structure of greigite, Fe_3S_4, *Eos Trans. AGU*, *71*, 1649.

Skinner, B. J., R. C. Erd, and F. S. Grimaldi (1964), Greigite, the thiospinel of iron: A new mineral, *Am. Mineral.*, *49*, 543–555.

Spender, M. R., J. M. D. Coey, and A. H. Morrish (1972), The magnetic properties and Mössbauer spectra of synthetic samples of Fe_3S_4, *Can. J. Phys.*, *50*, 2313–2326.

Szotek, Z., W. M. Temmerman, D. Ködderitzsch, A. Svane, L. Petit, and H. Winter (2006), Electronic structures of normal and inverse spinel ferrites from first principles, *Phys. Rev. B*, *74*, 174431, doi:10.1103/PhysRevB.74.174431.

Tang, Y., Q. W. Chen, Y. Xiong, and Y. Li (2007), Magnetic field-induced increase in conversion rate of Fe_3S_4 to FeS_2, *Chin. J. Inorg. Chem.*, *23*, 941–947.

Uda, M. (1965), On the synthesis of greigite, *Am. Mineral.*, *50*, 1487–1489.

Vandenberghe, R. E., E. De Grave, P. M. A. De Bakker, M. Krs, and J. J. Hus (1992), Mössbauer effect study of natural greigite, *Hyperfine Interact.*, *68*, 319–322, doi:10.1007/BF02396500.

van Dongen, B. E., A. P. Roberts, S. Schouten, W. T. Jiang, F. Florindo, and R. D. Pancost (2007), Formation of iron sulfide nodules during anaerobic oxidation of methane, *Geochim. Cosmochim. Acta*, *71*, 5155–5167, doi:10.1016/j.gca.2007.08.019.

Walz, F. (2002), The Verwey transition—A topical review, *J. Phys. Condens. Matter*, *14*, R285–R340, doi:10.1088/0953-8984/14/12/203.

Wright, J. P., J. P. Attfield, and P. G. Radaelli (2001), Long range charge ordering in magnetite below the Verwey transition, *Phys. Rev. Lett.*, *87*, 266401, doi:10.1103/PhysRevLett.87.266401.

Wright, J. P., J. P. Attfield, and P. G. Radaelli (2002), Charge ordered structure of magnetite below the Verwey transition, *Phys. Rev. B*, *66*, 214422, doi:10.1103/PhysRevB.66.214422.

Yamaguchi, S., and H. Wada (1970), Magnetic anisotropy of Fe_3S_4 as revealed by electron diffraction, *J. Appl. Phys.*, *41*, 1873–1874, doi:10.1063/1.1659128.

Zhang, Z., and S. Satpathy (1991), Electron states, magnetism, and the Verwey transition in magnetite, *Phys. Rev. B*, *44*, 13,319–13,331, doi:10.1103/PhysRevB.44.13319.

L. Chang and A. P. Roberts, National Oceanography Centre, University of Southampton, European Way, Southampton SO14 3ZH, UK. (liao.chang@noc.soton.ac.uk)

Q. Chen and Y. Tang, Hefei National Laboratory for Physical Sciences at Microscale and Department of Materials Science and Engineering, University of Science and Technology of China, Hefei 230026, China.

B. D. Rainford, School of Physics and Astronomy, University of Southampton, Southampton SO17 1BJ, UK.

C. Ritter and J. R. Stewart, Institut Laue-Langevin, 6 rue Jules Horowitz, F-38042 Grenoble, France.